IEEE Access
Multidisciplinary ⋮ Rapid Review ⋮ Open Access Journal

Received December 25, 2019, accepted January 14, 2020, date of publication February 4, 2020, date of current version February 11, 2020.

Digital Object Identifier 10.1109/ACCESS.2020.2971634

Simulation on Deposition Characteristics of Contamination Particles in Fog-Haze Environment

YUKUN LV[1], WEIPING ZHAO[1,2], AND QINGZHUANG SONG[1]

[1]Department of Power Engineering, North China Electric Power University, Baoding 071003, China
[2]School of Energy, Power and Mechanical Engineering, North China Electric Power University, Beijing 102206, China

Corresponding author: Weiping Zhao (weiping_zhao@ncepu.edu.cn)

ABSTRACT Fog-haze weather can aggravate the particles deposition on the insulator surface, which will cause pollution flashover. In this paper, the multiphysics software COMSOL was used to numerically simulate the particle deposition characteristics on the surface of XWP_2-160 porcelain insulator under wind tunnel conditions, and the simulation results were compared with wind tunnel test results to verify the rationality of the simulation model and the method. Based on this, the contamination deposition characteristics of this insulator on 110kV transmission lines under fog-haze environment were simulated. And the effects of wind speed, contamination concentration, and voltage type on particle deposition were analyzed. The results show that under the same conditions, the *NSDD* under DC voltage is the largest and it is the smallest under unelectrified state. The particle deposit amount increases approximately linearly with increasing wind speed and contamination concentration under DC voltage. In moderate fog-haze, the influence of wind speed on AC transmission line is larger than that on DC transmission line. The proportion of $NSDD_{DC}$ to $NSDD_{AC}$ displays a trend of gradual decrease with increasing wind speed and tends to be gentle gradually, and the ratio under all conditions is greater than 4.

INDEX TERMS Fog-haze environment, particle deposition characteristics, wind speed, contamination concentration, voltage type.

I. INTRODUCTION

Dust deposition on insulator is a hydrodynamic process of contamination particles hitting the insulator, and its performance is directly related to the safe and stable operation of power system [1]–[3]. In recent years, fog-haze weather appears frequently in some regions of our country with the rapid development of China's industry. In general, the high incidence period of fog-haze weather is mainly in autumn and winter, especially in cold winter, so the fog in fog-haze weather mentioned in this paper refers to cold fog. The fog-haze weather can aggravate the deposition of contamination particles on the surface of insulator, and then incur pollution flashover [4]–[6]. Therefore, it is of great significance to research the deposition characteristics of contamination particle on the insulator surface in fog-haze environment.

Previously, numerous researches on the particle deposition characteristics on the surface of insulators have been carried out and many important conclusions have been drawn. Qiao *et al.* [7] defined the pollution ratio k as the ratio of *NSDD* under DC voltage and unelectrified state, and studied the change of k under different environmental parameters by wind tunnel test and numerical simulation. The results show that k increases with increasing electrical stress and decreases with the increase of wind speed. Zhang *et al.* [8] experimentally studied the pollution distribution on different positions of the insulator surface, and pointed out that the pollution on the upper and lower surface, as well as the upside and leeward side of the insulator showed an uneven distribution. With the decrease of the particle size, the pollution non-uniformity coefficient $K_{T/B}$ (the ratio of *NSDD* on the upper and lower surface of insulator) and $K_{W/L}$ (the ratio of *NSDD* on the upside and leeward side) both decreased. Ref. [9] explored the salt deposition and surface flashover mechanism of high voltage insulators near the shoreline, which has a certain guiding significance for the research of *ESDD*. However, judging from the occurrence of fog-haze weather in some areas of China in recent years, especially in North China, the pollution particles deposited on the insulator surface come from a wide range of sources, such as particles emitted by

The associate editor coordinating the review of this manuscript and approving it for publication was Poki Chen.

coal-fired power plants, or produced by construction and farmland straw combustion as well as vehicle emissions, etc. And its main composition is insoluble pollutants rather than sea salt. Therefore, this paper focuses on the deposition process of insoluble pollutants (*NSDD*) on the insulator surface. Generally speaking, the deposition of pollution particles is mainly determined by two forces: one is the force that makes the particles move to the surface of the insulator; the other is the force that makes the particles deposit on the surface of the insulator without falling off. These two forces provide the motive force for the movement of the contaminated particles, and urge them to collide with the insulator surface, and then adhere and deposit. In the natural environment, pollution particles carried by the incoming air move to the insulator under the combined action of gravity force, fluid drag force, and electric field force. In the process of collision and adhesion between particles and insulator surface, in addition to the above three forces, particles will also be affected by collision force, adhesion force, and friction force. It is the combined action of these forces that leads to the deposition of particles.

In addition, as far as the size of deposited particles is concerned, the particles diameter on the insulator surface is generally smaller than 50 μm in the natural environment [10], [11]. However, in the fog-haze environment, the particles deposited on the surface of porcelain insulator have a particle size of smaller than 14.6 μm and account for about 90% [12]. The particle size has a significant effect on particles contamination deposition on the insulator surface [13]–[15]: the movement trajectory of contamination particles smaller than 10μm mainly depends on electric field force, while the function of fluid drag force is more conspicuous when the diameter is larger than 10 μm [16].

The influence of fog-haze weather on the external insulation of power equipment is mainly manifested in two aspects: on the one hand, the influence of fog, that is, humidity, which is one of the necessary conditions for causing the insulation layer to get wet and causing pollution flashover [17]. On the other hand, the influence of haze,that is, the effects of pollution particles in the atmosphere. Haze increases the deposit amount of contamination particles on the external insulation surface of power system equipment, and is likely to cause pollution flashover after superimposed with high humid environment [18]. However, there are few researches on the contamination particles deposition characteristics on the surface of insulator under fog-haze weather. The literature [3], [4], [19] demonstrated that wet deposition caused by gravity in fog-haze environment significantly aggravates the contamination deposition on the insulator surface. But the high concentration of PM2.5 has a very extremely limited contribution to the increase of particle deposit amount. Sun *et al.* [20] experimentally studied the deposition characteristics of contamination particles on different types of insulators. The results showed that the deposit amount of particles on each insulator surface increased significantly in a short time under fog-haze environment, and the contamination deposit amount on composite insulator was more serious than that of porcelain and glass insulators.

As for research method, predecessors have mostly used experiment to explore the deposition characteristics of contamination particles on the insulator surface in fog-haze environment. However, there are few reports on the research of contamination deposition characteristics based on numerical simulation, especially the related deposition mechanisms of particles needs to be deepened. Based on mechanics and energy mechanism, Lv *et al.* [21], [22] obtained the deposition criterion of contamination particles on the insulator surface at low wind speed. The criterion reasonably explains the collision and deposition of particles on the insulator surface, which has certain guiding significance. Hussain *et al.* [23] experimentally studied the effect of wind speed on *ESDD* and *NSDD* on the insulator surface, and pointed out that when the wind speed is not greater than 8m/s, the particle deposition rate increases with the increase of wind speed. When wind speed is greater than 8m/s, the particle deposition rate decreases with increasing wind speed.

What's more, compared with test method, the numerical simulation has the advantages of shorter time and lower cost, and the effect of single factor on the deposition characteristics of contamination particles also can be obtained. In this paper, the XWP_2-160 porcelain insulator was taken as research object. The COMSOL Multiphysics software was employed to simulate the deposition characteristics of contamination particles on the insulator surface under wind tunnel condition, and the simulation results was compared with the wind tunnel test results to verify the rationality of simulation model and method. Based on this, the deposition characteristics of particles on insulators under fog-haze environment was studied, and the effects of several factors such as wind speed, contamination concentration, and voltage type on particles deposition were analyzed.

II. MATHEMATICAL MODEL AND CONTROL EQUATION

The deposition of contamination particles on the insulator surface is the result of synthetic function of several physical fields such as flow field, electric field, and particle field. The methods for describing fluid motion include Lagrangian method and Eulerian method. Among them, the Lagrangian method takes a single fluid particle as the research object, and calculates the particle trajectory by solving the motion equation of each particle. However, the Euler method uses each spatial position in the flow field as the research object to describe the change of the physical parameters of the fluid particle over time in the spatial position [24], [25]. In the research of particle motion and deposition process, it is necessary to grasp the movement of particle point at each moment. Therefore, the Lagrangian method is employed in this paper to describe the particles movement. In the gas-solid two-phase flow composed of particles and air, air is regarded as continuous phase and the turbulence model is used to simulate the distribution of flow field around the insulator.

The contamination particles are regarded as discrete phase, and the fluid flow particle tracking model is used to simulate the movement trajectory of particles.

A. MATHEMATICAL MODEL OF FLOW FIELD AND CONTROL EQUATION

Viscosity is an important property of fluid anti-deformation, and the actual fluid in nature is viscous. For air, as a viscous fluid, its velocity is small when it flows near the insulator (in fog-haze environment, the wind speed is generally less than 3m/s). Besides, the pressure changes little and the change of density can also be ignored. Accordingly, in the analysis and calculation of the flow field, the air flowing through the insulator can be regarded as an incompressible viscous fluid. Considering that airflow bends easily when flowing on the insulator surface, the RANS k-ε model [26] is adopted. The control equation is expressed in Eq. (1).

$$\begin{cases} \rho_0(\boldsymbol{U}\cdot\nabla)\boldsymbol{U} \\ \quad = \nabla\cdot\left[-p\boldsymbol{I}+(\mu+\mu_T)\left(\nabla\boldsymbol{U}+(\nabla\boldsymbol{U})^T\right)-\dfrac{2}{3}\rho_0 k\boldsymbol{I}\right]+\boldsymbol{F} \\ \nabla\cdot\boldsymbol{U}=0 \\ \rho_0(\boldsymbol{U}\cdot\nabla)k=\nabla\cdot\left[\left(\mu+\dfrac{\mu_T}{\sigma_k}\right)\nabla k\right]+p_k-\rho_0\varepsilon \\ \rho_0(\boldsymbol{U}\cdot\nabla)\varepsilon=\nabla\cdot\left[\left(\mu+\dfrac{\mu_T}{\sigma_e}\right)\nabla\varepsilon\right]+C_{\varepsilon1}\dfrac{\varepsilon}{k}p_k-C_{\varepsilon2}\rho_0\dfrac{\varepsilon^2}{k} \\ \mu_T=\rho_0 C_\mu\dfrac{k^2}{\varepsilon} \\ p_k=\mu_T\left[\nabla\boldsymbol{U}:\left(\nabla\boldsymbol{U}+(\nabla\boldsymbol{U})^T\right)\right] \end{cases} \tag{1}$$

where $\boldsymbol{U}$ is the velocity of flow field, m/s; $\boldsymbol{I}$ is the tensor of principal stress, Pa; μ_{T} and μ are respectively the dynamic viscosity of turbulence and the dynamic viscosity of air, Pa·s; ρ_0 is the density of air, kg/m^3; $\boldsymbol{F}$ is volume force, N/m^3; k is turbulence energy, m^2/s^2; ε is dissipation rate of turbulence, m^2/s^3; C_μ, σ_k, σ_ε, $C_{\varepsilon1}$, $C_{\varepsilon2}$ are the model parameters of turbulence; and p_k is turbulent energy term, W/m^3.

B. MATHEMATICAL MODEL OF ELECTRIC FIELD AND CONTROL EQUATION

In the model of electric field, the uppermost iron cap of the insulator string is used as the ground terminal, and the lowermost steel leg is selected as the high-voltage terminal, and the corresponding voltage levels are applied respectively. In addition, during the simulation, an ''infinite element domain'' with a certain thickness is constructed as an electromagnetic wave absorption region on the outer boundary of the calculation area, and is set as electrical insulation boundary condition. The boundary condition settings of the electric field module are described in detail in Section III (C) ''Single-Value Conditions Setting'' and Figure 1c. In the simulation, steady-state analysis is done on DC electric field. The control equation [22] is expressed as follows:

$$\begin{cases} \nabla\cdot\boldsymbol{D}=\rho_v \\ \boldsymbol{E}=-\nabla\boldsymbol{V} \\ \boldsymbol{D}=\varepsilon_0\varepsilon_0'\boldsymbol{E} \end{cases} \tag{2}$$

where $\boldsymbol{D}$ is electric displacement intensity, C/m^2; $\boldsymbol{E}$ is electric field strength, V/m; $\boldsymbol{V}$ is electric potential, V; ε_0 is vacuum dielectric constant, F/m; ε_0' is relative dielectric constant of material; ρ_{v} is volume charge density, C/m^3.

Frequency-domain analysis is done on AC electric field, and its control equation is as follows:

$$\begin{cases} \nabla\cdot\boldsymbol{J}=Q_j \\ \boldsymbol{E}=-\nabla\boldsymbol{V} \\ \boldsymbol{J}=\sigma\boldsymbol{E}+\boldsymbol{J}_e \end{cases} \tag{3}$$

where $\boldsymbol{J}$ is total current density, A/m^2; Q_{j} is charge quantity, C; σ is electric conductivity, S/m; $\boldsymbol{J}_{\mathrm{e}}$ is external current density, A/m^2.

C. MATHEMATICAL MODEL OF PARTICLE FIELD AND CONTROL EQUATION

In the establishment of particle field model, the treatment of polluted particles and its force analysis are the basis for the successful numerical simulation. Due to the different shapes of pollution particles in nature, it is difficult to describe them by mathematical method, and the collision and deposition process between particles and insulator surface is quite complex. Therefore, in the numerical simulation, the contamination particles are equivalent and simplified as follows: the contamination particles are equivalent to spherical particles and the contact between them and the insulator surface conforms to the JKR contact model [27]; the initial speed of particles is same as the speed of flow field; the small forces on particles such as the dielectrophoresis force, thermal electrophoresis force, and the interaction force between particles are ignored; the gravity force F_{g}, electric field force F_{e}, and fluid drag force F_{d} are only considered during the movement of pollution particles [15], [16]. The particle movement process can be described as:

$$\begin{cases} \dfrac{\mathrm{m}_p d\boldsymbol{v}}{d\boldsymbol{t}}=\boldsymbol{F}_{\mathrm{g}}+\boldsymbol{F}_{\mathrm{e}}+\boldsymbol{F}_{\mathrm{d}} \\ \boldsymbol{F}_{\mathrm{g}}=\mathrm{m}_p\boldsymbol{g} \\ \boldsymbol{F}_{\mathrm{e}}=\boldsymbol{e}Z\boldsymbol{E} \\ Z=\dfrac{\pi\boldsymbol{d}_{\mathrm{p}}^3\rho_{\mathrm{p}}\boldsymbol{Q}}{6\boldsymbol{e}} \\ \boldsymbol{F}_{\mathrm{d}}=\dfrac{1}{\tau_{\mathrm{p}}}\mathrm{m}_p(\boldsymbol{U}-\boldsymbol{v}) \\ \mathrm{C_D}=\dfrac{24}{Re_{\mathrm{r}}}(1+0.15Re_{\mathrm{r}}^{0.687}) \end{cases} \tag{4}$$

where m_{p} is the mass of a single contamination particle, kg; $\boldsymbol{t}$ is particle movement time, s; $\boldsymbol{v}$ and $\boldsymbol{U}$ are respectively the particle velocity and the velocity of flow field, m/s; e is the charge quantity of the elementary charge, C; Z is the charge number of particle; d_{p} is the particle diameter, m; ρ_{p} is the

TABLE 1. Main parameters of XWP_2-160 porcelain double-umbrella insulator.

Parameters	Value
Structural height/(mm)	155
Creepage distance/(mm)	450
Shed diameter/(mm)	300

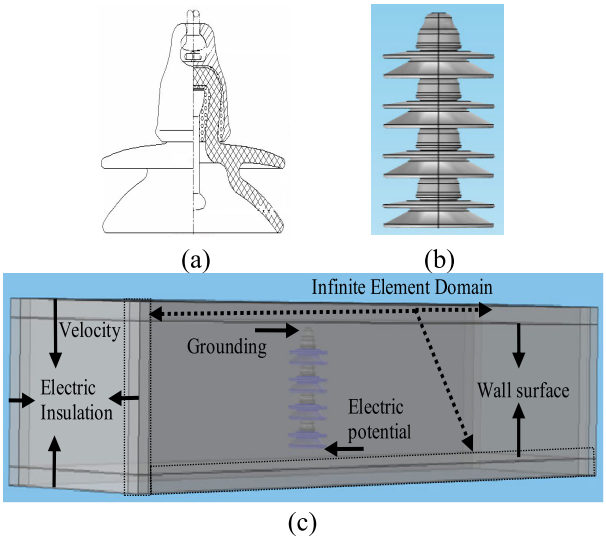

FIGURE 1. The model of insulator and boundary conditions setting. (a) The structure schematic diagram of insulator, (b) Simplified simulation model of insulator, and (c) Boundary conditions setting for wind tunnel contamination accumulation.

particle density, kg/m^3; Q is the charge quantity of a particle per unit weight, C/kg; τ_p is the response time of particle in the flow field, s;C_D is the drag coefficient; and Re_r is Reynolds number.

III. WIND TUNNEL TEST AND SIMULATION RESULTS ANALYSIS

A. WIND TUNNEL TEST AND ITS METHOD

Wind tunnel test [28] is operated at low speed section (10.5 m×1.1 m×0.8 m). As the research project comes from program of State Grid Corporation of China, the test wind speed is required to be the natural breeze environment 4m/s. Therefore, the wind speed of 4 m/s is chosen. The design parameters of XWP_2-160 porcelain insulator selected in the test are listed in Table 1, and structure schematic diagram is shown in Figure 1a.

Limited by the height of the wind tunnel laboratory, an insulator string of four pieces is selected as the test research object. During wind tunnel test, the upper end of insulator is the grounding end and the lower end is high-voltage end. The test voltage is DC voltage, i.e. 0, ±12, ±18, ±24, ±30, ±36 kV. Diatomite with low density and NaCl with less quantity can be blown up because of low wind speed in the test. Therefore, the non-soluble deposit density (*NSDD*) is selected as the evaluation standard of particle deposit amount on the insulator surface. The main parameters of contamination samples for wind tunnel test are listed in Table 2.

TABLE 2. Main parameters of contamination sample.

Parameter	Fine sand	Diatomite	NaCl
Particle Diameter/(μm)	100	50	100
Density/(g/cm^3)	2.32	0.47	2.165
Proportion	6	6	1

TABLE 3. Comparison of simulation and test results of wind tunnel pollution under different mesh number.

mesh number	-30kV		30kV	
	simulation time	error with test result	simulation time	error with test result
498,846	6hours and 56minutes	14.67%	6hours and 34minutes	15.31%
728,303	**8hours and 12minutes**	**10.99%**	**7hours and 48minutes**	**13.57%**
901,315	10hours and 28minutes	11.25%	10hours and 16minutes	15.66%
1,200,356	11hours and 54minutes	10.34%	11hours and 37minutes	12.89%

B. PHYSICAL MODEL BUILDING

In the software COMSOL, a computational domain (Figure 1c) in the same size as the low speed section of wind tunnel laboratory is built. The simplified model of the porcelain double-umbrella insulator used during the simulation is shown in Figure 1b. The grid irrelevance verification of the model is a necessary step of numerical simulation. So, the simulation results under ±30kV DC voltage are taken as an example to illustrate the grid independence verification, as shown in Table 3. According to the verification results in Table 3, when the mesh number of the porcelain double-umbrella insulator is 728,303, about 730 thousand, it can better meet the requirements of calculation accuracy and calculation time.

C. SINGLE-VALUE CONDITIONS SETTING

1) BOUNDARY CONDITIONS SETTING

In the flow field, the inlet is set to be velocity inlet (4 m/s) and the outlet is set to be pressure outlet. In the electric field, an infinite element domain is set as the default electrical insulation boundary condition to absorb the electromagnetic wave (as shown in Figure 1c). Besides, the setting of high-voltage end and grounding end is as same as that in wind tunnel test. In the fluid flow particle tracking field, the particles are released from the inlet. When they collide with the surface of insulators, judgment is made. If the sedimentary conditions are met, contaminated particles will deposit on the surface of insulators; otherwise, it will rebound [26].

2) MATERIAL PARAMETERS SETTING

Porcelain insulator is comprised of steel leg, iron hat, and sheds. The material property of steel leg and iron hat is cast

TABLE 4. Material parameters setting.

Parameter	Iron	Porcelain	Wet air
Relative dielectric constant	1×10^{7}	5.5	1.0007
Density/(kg/m^3)	Default	Default	1.185
Dynamic viscosity/(Pa·s)	Default	Default	1.842×10^{-5}

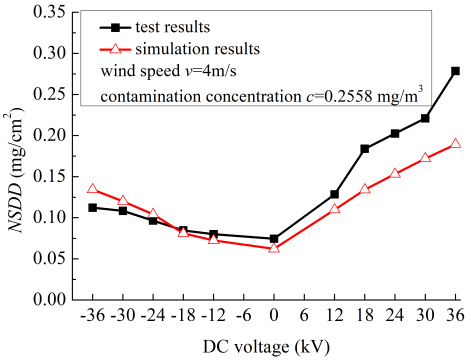

FIGURE 2. Comparison of simulation results with test results.

iron while the shed is set by self-definition. Referring to wind tunnel test, the material property of computational domain of flow field is set to be wet air at relative humidity 76%. The detailed parameter settings are listed in Table 4.

3) ANALYSIS OF SIMULATION RESULTS AND TEST RESULTS

In the wind tunnel test, the particle deposit amount on the surface of porcelain double-umbrella insulator reached saturation at 15 hours. When measuring the deposit amount of particles, each experiment was repeated five times, and then averaged to reduce the error caused by the human operation. Similarly, in the wind tunnel pollution simulation, each simulation condition is also repeated for 5 times and its average value is taken. In addition, the particle deposit amount (i.e. *NSDD*, mg/cm^2) needs to be converted into the deposit amount of the insulator during the whole saturation time. The equation [26] is as follows:

$$\mathrm{NSDD} = \xi \frac{n m_{\mathrm{p}} t_{\mathrm{s}}}{t_{\mathrm{p}} S} \tag{5}$$

where ξ is time coefficient; n is the total number of contamination particles deposited on the insulator skirt surface; S is the total surface area of insulator umbrella skirt, m^2; t_s is the wind tunnel test time, s; t_{p} is the time of wind tunnel pollution simulation, s.

Figure 2 indicates the NSDD of simulation results and wind tunnel test results are at the same level and the variation trend is similar and consistent. Although there is error between simulation results and test results, the simulation results can almost accurately reflect the contamination particles deposition status on the surface of insulators. This verifies the rationality of numerical simulation method and model. Therefore, it is feasible to research the deposition characteristics of contamination particles on the insulator surface using the simulation model established by COMSOL.

IV. SIMULATION AND RESULT ANALYSIS OF DEPOSITION CHARACTERISTICS OF PARTICLES IN FOG-HAZE WEATHER

A. SIMULATION OF CONTAMINATION PARTICLE DEPOSITION

Usually, fog-haze weather happens in the environmental conditions of low wind speed and high humidity. In this environment, the main particles of contamination are PM2.5 and PM10. However, the high-concentration PM2.5 has a very extremely limited contribution to the increase of particle deposit amount on insulator surface [3]. Limited by computing resource, this paper mainly studies the effect of concentration of PM10 on the deposition characteristics of contamination particles. In addition, the effects of wind speed and voltage types (DC voltage, AC voltage, and unelectrified state) on particle deposition will also be studied in this section.

According to the characteristics of the fog-haze weather, the relative humidity (*RH*) of air is set to be 80%. According to the method of humidity setting in Ref. [26], the air parameters (such as relative dielectric constant, viscosity, and density of the air) as well as the capillary force and van der Waals force are calculated and set in the boundary conditions. During the simulation calculation, it is considered that each physical parameter corresponds to a relative humidity. Besides, wind speed is set as 1-3 m/s and the diameter of contamination particles is 10 μ. Referring to the daily average standard of PM10 (0.15 mg/m^3) in the national standard [29], combined with the actual environmental conditions, 1-3 times of the standard is used in simulation research as the standard of contamination concentration: mild fog-haze (i.e. c = 0.15 mg/m^3), moderate fog-haze (i.e. c = 0.3 mg/m^3), and severe fog-haze (i.e. c = 0.45 mg/m^3). Since the contamination concentration characterizes the total mass of pollution particles in a unit volume. Therefore, the number of particles at a contamination concentration can be calculated according to the ratio of the total mass of pollution particles to the mass of a single particle. In the simulation, the contamination concentration can be reflected by the number of pollution particles. In addition, the setting of boundary conditions and material parameters is similar to that in wind tunnel simulation model. According to the 110 kV voltage level, a string of seven pieces insulator is selected, as shown in Figure 3. To reduce the error, each of the simulation conditions is repeated five times, and then averaged. Similar to wind tunnel pollution simulation, the *NSDD* is still selected as the evaluation index of particle deposition characteristics in fog-haze environment.

B. ANALYSIS OF MULTIPHYSIS SIMULATION RESULTS

1) FLOW FIELD SIMULATION RESULTS

Taking the wind speed of 3 m/s and the particle size of 10μm unde DC voltage as an example, the simulation results of flow field are analyzed, as shown in Figure 4.

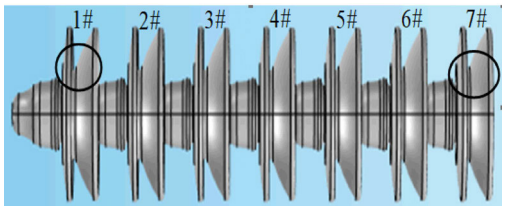

FIGURE 3. Insulator string and skirt number.

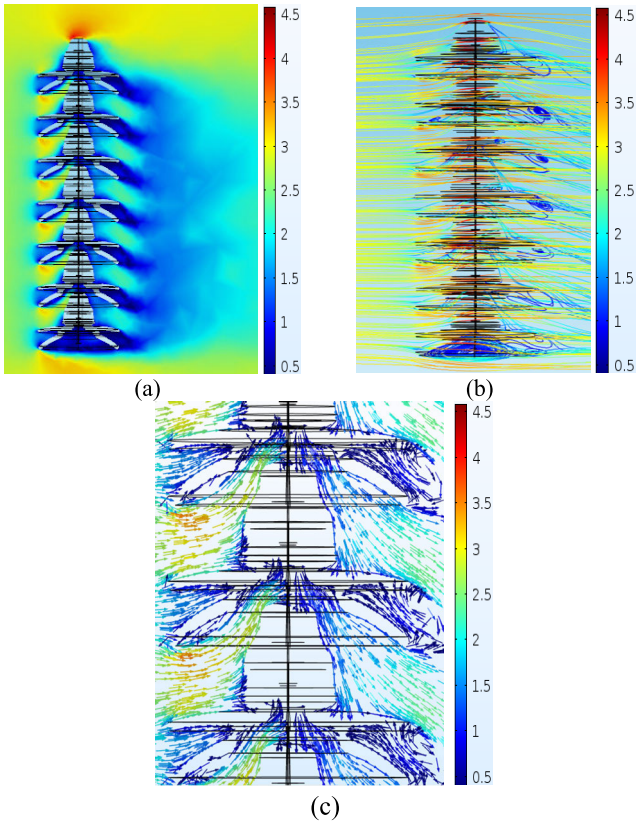

FIGURE 4. Flow field simulation results. (a) Contours of velocity magnitude, (b) Pathlines of velocity magnitude, and (c) Velocity vector diagram.

It can be noticed from Figure 4a that when wind speed is 3 m/s and the airflow flows through the insulator surface, a boundary layer of a certain thickness is formed on the leeward side of insulator because of the fluid viscosity, and a boundary layer separation phenomenon occurs. On the windward side of the insulator, especially between the lower insulator skirt and the iron cap of the underlying insulator, the airflow velocity approaches or exceeds the wind speed, while at the insulator surface it is approximately zero.

Figure 4b and 4c indicate that when the airflow passes through insulator surface, vortex is formed between the upper and lower umbrella skirts of the insulator on the leeward side, and the turbulent pulsation is relatively strong. In addition, when the airflow passes through the bottom skirt, a large counterclockwise vortex will be formed on the lower skirt surface due to the flow around effect. The simulation results of flow field are consistent with the theory of viscous fluid mechanics, indicating that the flow field simulation results are reasonable.

2) ELECTRIC FIELD SIMULATION RESULTS

Figure 5 demonstrates the electric potential plot and the spatial electric field line distribution under DC and AC voltage when particle size is 10 μm and wind speed is 3 m/s.

It can be observed from Figure 5a and 5b that under DC and AC voltage, the potential of each insulator skirt decreases sequentially from the electric potential end to the grounding end. That is, the maximum potential at each voltage appears at the steel foot of the 7# insulator skirt, and the minimum potential appears at the iron cap of 1# insulator skirt. Compared with Figure 5c and 5d, it can be seen that the distribution of the electric field line is denser near the insulator string. Otherwise, the electric field line is sparse. And the electric field is approximately "U" distribution along the umbrella skirt. This is also in line with the electromagnetic field theory, indicating that the simulation of the electric field is reasonable.

C. SIMULATION RESULT ANALYSIS OF PARTICLE DEPOSITION CHARACTERISTICS ON INSULATOR SURFACE

1) THE INFLUENCE OF WIND SPEED ON CONTAMINATION PARTICLE DEPOSITION

Figure 6 illustrates the variation of *NSDD* with wind speed under DC, AC voltage, and unelectrified state.

Figure 6a indicates the *NSDD* at different contamination concentration increases linearly approximately with the increase of wind speed under DC voltage. And at the same wind speed, the higher the contamination concentration, the greater the *NSDD*.

It can be seen from the Figure 6b that the *NSDD* increases with increasing wind speed under AC voltage. However, when the speed is greater than 1.5 m/s, the *NSDD* reaches the largest when the contamination concentration is 0.3 mg/m^3 at the same wind speed, while the smallest at the concentration of 0.15 mg/m^3.

It can be noticed from Figure 6c that under unelectrified state, the *NSDD* firstly decreases and then increases when the contamination concentration is 0.15 mg/m^3 and 0.45 mg/m^3, and reaches the minimum at the wind speed of 2 m/s. However, the *NSDD* increases with increasing wind speed when the contamination concentration is 0.3 mg/m^3. When the wind speed is about 1.3-2.8 m/s and the contamination concentration is 0.3 mg/m^3, the *NSDD* is larger than those under the concentration of 0.15 mg/m^3 and 0.45 mg/m^3.

Compared to the subgraphs in Figure 6, the *NSDD* increases approximately linearly with the increase of wind speed under DC and AC voltage at the same contamination concentration. The fluid drag force exerted on contamination particles increases with increasing wind speed, which greatly increases the probability of collision between contamination

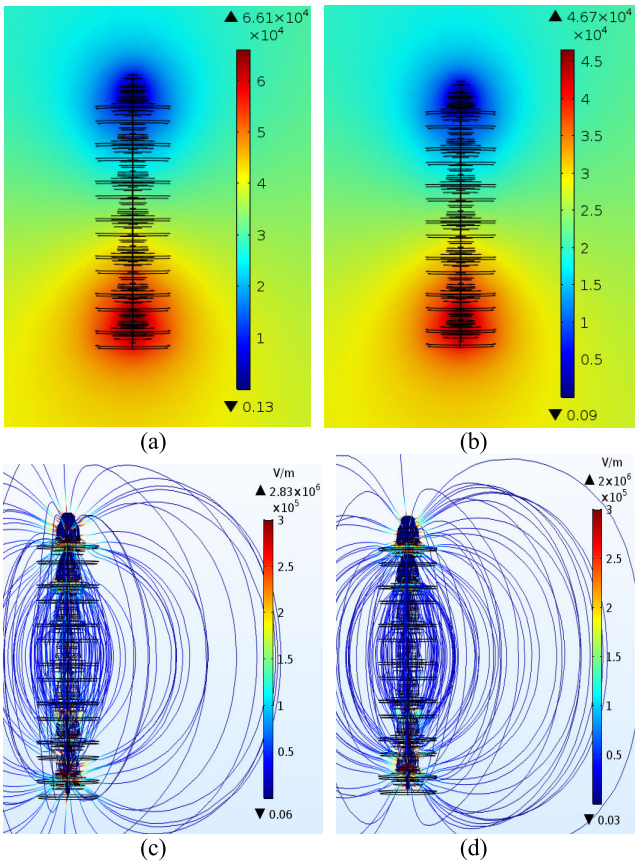

FIGURE 5. The potential plot and spatial electric field line distribution under DC and AC voltage. (a) DC potential plot, (b) AC potential plot, (c) Spatial electric field line distribution under DC voltage, and (d) Spatial electric field line distribution under AC voltage.

particles and insulator surface. In addition, the turbulent fluctuations around the insulator as well as the momentum and energy exchanges between particles and the flow field increase with increasing wind speed. As a result, the particles become more likely to collide with the insulator surface under the actions of the vortices and return to flow in the local flow field, resulting in an increase in *NSDD*.

Under the same condition, the contamination concentration has a great influence on the contamination deposit characteristic of the insulator. The increase of contamination concentration leads to an increase of contamination particles in unit volume, and hence, the probability of collision. Under unelectrified state, the contamination particles are mainly affected by the gravity and fluid drag force, and the existence of humidity and contamination concentration also has certain influence on the gas-solid two-phase flow composed of particles and air. When wind speed is about 1.3-2.8 m/s, the contamination concentration of 0.3 mg/m^3 may have a greater effect on contamination deposit than that of wind speed and humidity, so the *NSDD* at this concentration is the largest. When the wind speed exceeds this range, the higher the contamination concentration, the more complex the movement of particles in two-phase flow, so correspondingly, the *NSDD* is larger.

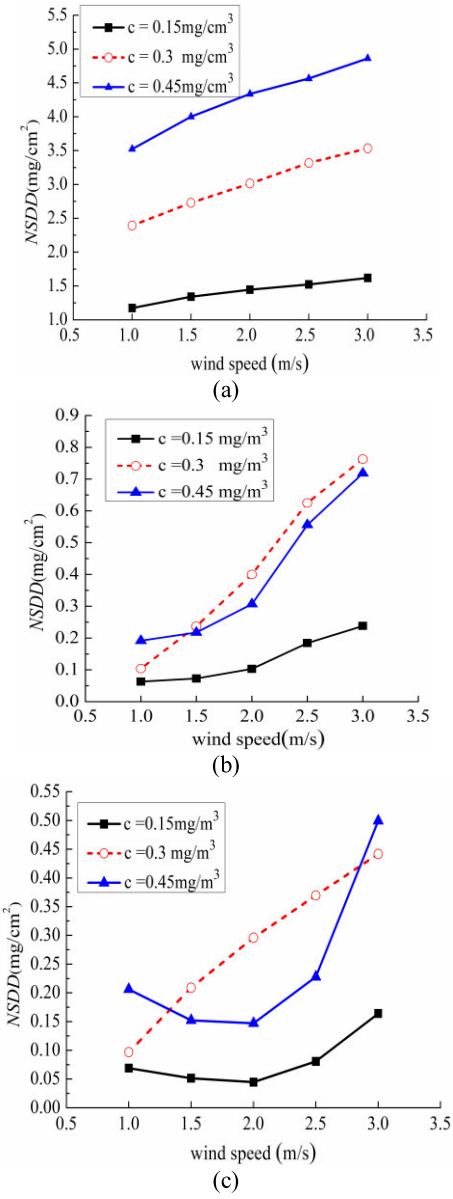

FIGURE 6. Relationship between *NSDD* and wind speed under different voltage types. (a) DC voltage, (b) AC voltage, and (c) Unelectrified state.

2) THE INFLUENCE OF CONTAMINATION CONCENTRATION ON PARTICLE DEPOSITION

The pollution concentration in the air has a significant impact on contamination particle accumulation on the insulator surface, and when combined with high-humidity environment, it will greatly increase the probability of pollution flashover accidents of insulators. Figure 7 shows the variation of the *NSDD* with contamination concentration under DC, AC voltage, and unelectrified state.

Figure 7 reveals that under DC voltage, the *NSDD* at different wind speed changes linearly with contamination concentration. However, under AC voltage, the *NSDD* increases with the increase of contamination concentration when wind speed is 1 m/s. At other wind speed, the *NSDD* firstly increases and then decreases, and reaches the maximum at the

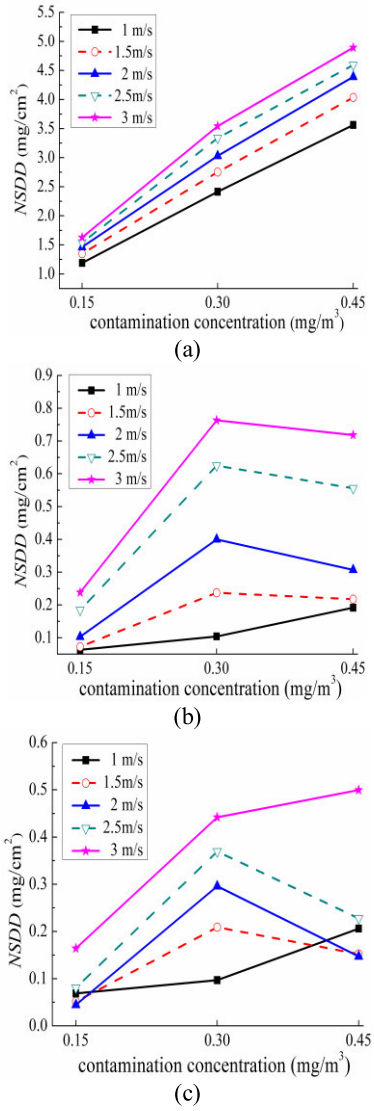

FIGURE 7. Relationship between the *NSDD* and contamination concentration under different voltage types. (a) DC voltage, (b) AC voltage, and (c) Unelectrified state.

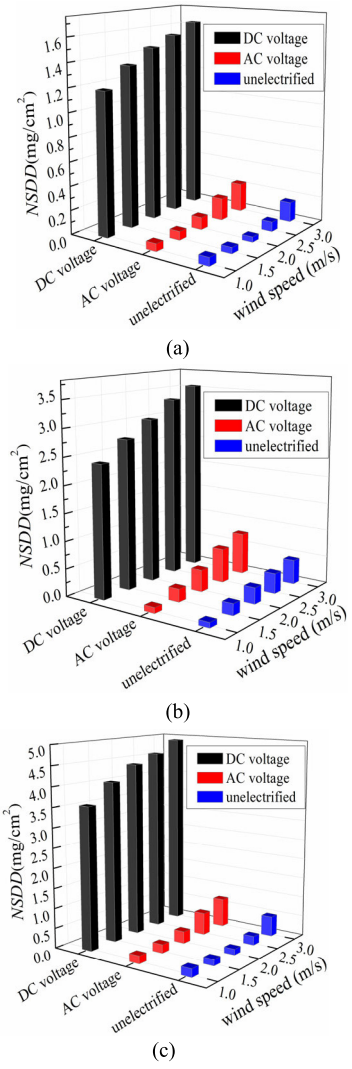

FIGURE 8. Relationship between the *NSDD* and voltage type under different contamination concentration. (a) $c = 0.15$ mg/m^3, (b) $c = 0.3$ mg/m^3, and (c) $c = 0.45$ mg/m^3.

contamination concentration of 0.3 mg/m^3. Under unelectrified state, the variation trend of *NSDD* with contamination concentration is similar to that under AC.

From the variation trend of Figure 7, it is found that under DC voltage, contamination particles are in the function of continuous electric field force. The increase of contamination concentration at each wind speed increases the probability of collision between particles and the insulator surface. Therefore, the *NSDD* is in approximate linear relation with contamination concentration, that is, the higher the degree of environment pollution, the greater the *NSDD*. Under AC voltage, the following performance of contamination particle is poor when wind speed is low (1 m/s), and it is easy to deposit under the combined action of periodical electric field force, fluid drag force, and gravity force. Therefore, the *NSDD* rises with the increase of contamination concentration at this wind speed. When the concentration is 0.3 mg/m^3, the coagulation effect of particles maybe the strongest, so the *NSDD* reaches the maximum.However, the change trend of *NSDD* under unelectrified state is similar to that under AC voltage. This is because when particles move in AC electric field, the effect of periodical electric field force on contamination particles is almost zero.

3) THE INFLUENCE OF VOLTAGE TYPE ON PARTICLE DEPOSITION

Figure 8 shows the relationship between *NSDD* and voltage type under different contamination concentration.

Figure 8 shows that at each wind speed and contamination concentration, the *NSDD* under DC voltage is the largest. When the contamination concentration is 0.15 mg/m^3, the *NSDD* is about 1.6 mg/cm^2. And when contamination concentration is 0.45 mg/m^3, the *NSDD* can reach up to 5 mg/cm^2. Under AC voltage, the maximum value of the *NSDD* is about 0.8 mg/cm^2 at each contamination

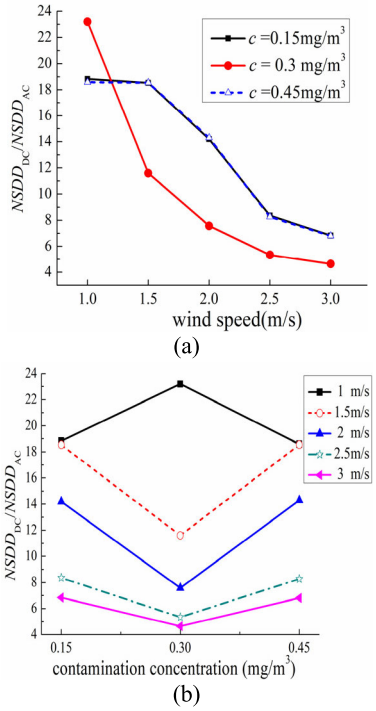

FIGURE 9. Proportion of $NSDD_{DC}$ to $NSDD_{AC}$ versus wind speed and contamination concentration curves. (a) Variation with wind speed, and (b) Variation with contamination concentration.

concentration and wind speed. However, under unelectrified state, the *NSDD* is slightly less than that of AC voltage.

Comparing the subgraphs in Figure 8, it can be seen that when either the contamination concentration or wind speed is constant, the *NSDD* increases with the increase of the other factor under DC voltage. When the contamination concentration does not change, the fluid drag force experienced by particles increase with increasing wind speed. In this case, the movement trajectory in flow field becomes more complex, and hence aggravates the change of electric field. Besides, at large wind speed, the effect of electric field force under DC voltage is more obvious, so the *NSDD* in the function of DC voltage is the largest. When wind speed does not change, the number of particles in unit volume increase with increasing contamination concentration, which further increases the collision probability between particles and insulator surface. Therefore, the *NSDD* under DC voltage increases as the contamination concentration increases at the same wind speed.

4) THE INFLUENCE OF WIND SPEED AND CONCENTRATION ON PROPORTION OF $NSDD_{DC}$ to $NSDD_{AC}$

The difference of contamination deposit amount between DC and AC voltage on transmission lines can not only be reflected directly from the quantity, but also can be expressed by the ratio of *NSDD* on insulator surface under the same condition, that is, the proportion of $NSDD_{DC}$ to $NSDD_{AC}$. Figure 9 demonstrates the variation trend of the proportion of $NSDD_{DC}$ to $NSDD_{AC}$ with wind speed and contamination concentration.

It can be observed from Figure 9 that the proportion of $NSDD_{DC}$ to $NSDD_{AC}$ displays a trend of gradual decrease with the increase of wind speed and tends to be gentle gradually. And the proportion under all conditions is greater than 4. It indicates that the influence of DC electric field gradually weakens with the increase of wind speed. Under DC and AC voltage, the difference of *NSDD* on the insulator surface decreases with increasing wind speed. When contamination concentration is 0.15 mg/m^3 and 0.45 mg/m^3, the proportion of $NSDD_{DC}$ to $NSDD_{AC}$ is almost the same. It indicates that the influence of wind speed on the ratio is basically the same in mild and severe pollution environment. When contamination concentration is 0.3 mg/m^3 and wind speed is larger than 1.5 m/s, the proportion of $NSDD_{DC}$ to $NSDD_{AC}$ is the smallest under each wind speed, indicating that the effect of wind speed on AC electric transmission line is larger than that on DC electric transmission line under moderate fog- haze environment. In addition, the data in the figure also demonstrates that in the polluted area where the pollution particle size is mainly 10 μm and the annual average wind speed is less than 3 m/s, if the contamination particle deposit amount is only considered, the selection of AC transmission line for 110 kV may be more conducive to reduce the probability of pollution flashover.

It is also can be drawn from Figure 9 that the proportion of $NSDD_{DC}$ to $NSDD_{AC}$ increases at first and then decreases with the increase of contamination concentration at the wind speed of 1 m/s. Under other wind speed, the ratio decreases at first and then increases with increasing concentration, and the minimum value is obtained at the concentration of 0.3 mg/m^3. This is mainly due to the interaction of various physical fields.

V. CONCLUSION

In this paper, the COMSOL Multiphysics software was applied to establish the pollution deposition model of XWP_2-160 porcelain insulator under wind tunnel conditions. The simulated results which were similar to test results were obtained, indicating the rationality of the simulation model and method. Based on the aforementioned method, the deposition characteristics of pollution particles on insulator surface under fog-haze environment were simulated. The effects of several factors such as wind speed, contamination concentration, and voltage type on particles deposition were analyzed. The followings are the main conclusions:

(1) Under the same conditions, the *NSDD* under DC voltage is the largest and it reaches the least under unelectrified state. The difference of *NSDD* between AC voltage and unelectrified state is small.

(2) The *NSDD* is approximately positively correlated with the contamination concentration under DC voltage. Under unelectrified state, the variation trend of *NSDD* with contamination concentration is similar to that under AC voltage.

(3) Under AC and DC voltage, the *NSDD* increases approximately linearly with increasing wind speed. However, under unelectrified state, the *NSDD* increases with the increase of wind speed in the moderate fog-haze environment, while

it firstly decreases and then increases as the wind speed increases in the mild and severe fog-haze.

(4) In the moderate fog-haze environment, the influence of wind speed on AC transmission line is larger than that on DC transmission line. The proportion of $NSDD_{DC}$ to $NSDD_{AC}$ displays a trend of gradual decrease with the increase of wind speed and the ratio is greater than 4 under each condition.

REFERENCES

[1] B. Zhang, J. He, R. Zeng, and X. Liang, "Voltage distribution along a long ceramic insulator string in a high-voltage tower window," *Compel*, vol. 29, no. 3, pp. 811–823, May 2010.
[2] J. Mahmoodi, M. Mirzaie, and A. A. Shayegani-Akmal, "Surface charge distribution analysis of polymeric insulator under AC and DC voltage based on numerical and experimental tests," *Int. J. Electr. Power Energy Syst.*, vol. 105, pp. 283–296, Feb. 2019.
[3] M. M. Hussain, S. Farokhi, S. G. Mcmeekin, and M. Farzaneh, "Effect of uneven wetting on E-field distribution along composite insulators," in *Proc. IEEE Electr. Insul. Conf. (EIC)*, Montreal, QC, Canada, Jun. 2016, pp. 69–72.
[4] C. Zhang, J. Hu, J. Li, D. Liu, L. Wang, and M. Lu, "Experimental study on the contamination deposition characteristics of insulators in a fog-haze environment," *IET Gener., Transmiss. Distrib.*, vol. 12, no. 2, pp. 406–413, Jan. 2018.
[5] Y. Guo, X. Jiang, Y. Liu, Z. Meng, and Z. Li, "AC flashover characteristics of insulators under haze-fog environment," *IET Gener., Transmiss. Distrib.*, vol. 10, no. 14, pp. 3563–3569, Nov. 2016.
[6] M. M. Hussain, S. Farokhi, S. G. Mcmeekin, and M. Farzaneh, "Effect of cold fog on leakage current characteristics of polluted insulators," in *Proc. Int. Conf. Condition Assessment Techn. Electr. Syst. (CATCON)*, Bangalore, India, Dec. 2016, pp. 163–167.
[7] X. Qiao, Z. Zhang, X. Jiang, and T. Liang, "Influence of DC electric fields on pollution of HVDC composite insulator short samples with different environmental parameters," *Energies*, vol. 12, no. 12, p. 2304, Jun. 2019.
[8] Z. Zhang, X. Qiao, S. Yang, and X. Jiang, "Non-uniform distribution of contamination on composite insulators in HVDC transmission lines," *Appl. Sci.*, vol. 8, no. 10, pp. 1962–1975, Oct. 2018.
[9] M. M. Hussain, M. A. Chaudhary, and A. Razaq, "Mechanism of saline deposition and surface flashover on high-voltage insulators near shoreline: Mathematical models and experimental validations," *Energies*, vol. 12, no. 19, pp. 3685–3704, Sep. 2019.
[10] Z. Y. Su and Y. S. Liu, "Comparison of natural contaminants accumulated on surfaces of suspension and post insulators with DC and AC stress in northern China's inland areas," *Power Syst. Technol.*, vol. 28, no. 10, pp. 13–17, May 2004.
[11] M. Zhang, R. Wang, L. Li, and Y. Jiang, "Size distribution of contamination particulate on porcelain insulators," *Coatings*, vol. 8, no. 10, pp. 339–357, Sep. 2018.
[12] Y. P. Tu, Y. F. Sun, Q. J. Peng, and C. Wang, "Particle size distribution characteristics of naturally polluted insulators under the fog-haze environment," *High Volt. Eng.*, vol. 40, no. 11, pp. 3318–3326, Nov. 2014.
[13] Y. Jiang, L. Li, M. Lu, R. Wang, Y. Jiang, S. Liu, and C. Su, "Statistical characteristics and mechanism analysis of adhered particle on surface under strong electric field," *Particuology*, vol. 43, pp. 110–122, Apr. 2019.
[14] Y. Liu, G. Wu, Y. Guo, X. Zhang, K. Liu, Y. Kang, and C. Shi, "Pollution agglomeration characteristics on insulator and its effect mechanism in DC electric field," *Int. J. Electr. Power Energy Syst.*, vol. 115, Feb. 2020, Art. no. 105447.
[15] Y. Lv, W. Zhao, J. Li, and Y. Zhang, "Simulation of contamination deposition on typical shed porcelain insulators," *Energies*, vol. 10, no. 7, pp. 1045–1057, Jul. 2017.
[16] M. Horenstein and J. Melcher, "Particle contamination of high voltage DC insulators below corona threshold," *IEEE Trans. Elect. Insul.*, vol. EI-14, no. 6, pp. 297–305, Dec. 1979.
[17] M. Farzaneh and O. Melo, "Properties and effect of freezing rain and winter fog on outline insulators," *Cold Regions Sci. Technol.*, vol. 19, no. 1, pp. 33–46, Dec. 1990.
[18] S. Gao, Z. C. Zhou, L. J. Yang, Y. Liu, F. B. Tao, and L. Zhang, "Factors contributing to haze and the influence on external insulation of power equipments," *Appl. Mech. Mater.*, vol. 700, pp. 631–636, Dec. 2014.
[19] S. Xu, C. Wu, S. H. Li, W. N. Bao, Y. Y. Liu, and X. D. Liang, "Research on pollution accumulation characteristics of insulators during fog-haze days," *Proc. CSEE*, vol. 37, pp. 2142–2150, Sep. 2017.
[20] Y. Sun, Y. Tu, C. Wang, S. Wang, Y. Cheng, Q. Peng, and X. Chen, "Contamination and AC pollution flashover characteristics of insulators under fog-haze environment," in *Proc. IEEE 11th Int. Conf. Properties Appl. Dielectric Mater. (ICPADM)*, Sydney, NSW, Australia, Jul. 2015, pp. 596–599.
[21] Y. Lv, J. Li, and W. Zhao, "Model optimization of pollution deposition criterion of insulators based on energy," *IEEE Trans. Dielectr. Electr. Insul.*, vol. 24, no. 5, pp. 2920–2929, Oct. 2017.
[22] Y. Lv, J. Li, X. Zhang, G. Pang, and Q. Liu, "Simulation study on pollution accumulation characteristics of XP13-160 porcelain suspension disc insulators," *IEEE Trans. Dielectr. Electr. Insul.*, vol. 23, no. 4, pp. 2196–2206, Aug. 2016.
[23] M. M. Hussain, S. Farokhi, S. G. Mcmeekin, and M. Farzaneh, "Impact of wind on pollution accumulation rate on outdoor insulators near shoreline," in *Proc. IEEE Int. Power Modulator High Voltage Conf. (IPMHVC)*, San Francisco, CA, USA, Jul. 2016, pp. 453–456.
[24] M. Rahimi-Gorji, O. Pourmehran, M. Gorji-Bandpy, and T. Gorji, "CFD simulation of airflow behavior and particle transport and deposition in different breathing conditions through the realistic model of human airways," *J. Mol. Liquids*, vol. 209, pp. 121–133, Sep. 2015.
[25] Q. Huang, Y. Zhang, Q. Yao, and S. Li, "Numerical and experimental study on the deposition of fine particulate matter during the combustion of pulverized lignite coal in a 25 kW combustor," *Powder Technol.*, vol. 317, pp. 449–457, Jul. 2017.
[26] Y. Lv, W. Zhao, W. Yan, and Y. Liu, "Optimization of the contamination particle deposition model based on humidity and surface energy," *Appl. Thermal Eng.*, vol. 157, Jul. 2019, Art. no. 113734.
[27] G. Liu, S. Li, and Q. Yao, "A JKR-based dynamic model for the impact of micro-particle with a flat surface," *Powder Technol.*, vol. 207, nos. 1–3, pp. 215–223, Feb. 2011.
[28] F. C. Lv, H. Huang, and Y. P. Liu, "Contamination depositing characteristics of insulators under natural crosswind conditions with wind tunnel simulation," *High Volt. Eng.*, vol. 40, no. 5, pp. 1281–1289, May 2014.
[29] *GB 3095-2012 Environmental Air Quality Standard*, Beijing, China: Environmental Science Publishing House, Feb. 2012.

YUKUN LV received the B.S. and M.S. degrees from North China Electric Power University, in 1987 and 1994, respectively. He is currently an Associate Professor with the Department of Power Engineering, North China Electric Power University, Baoding, China. His special fields of interests include the high-voltage transmission lines safety and insulation, contamination deposition characteristics of insulators, and economic analysis of thermal equipment and large-scale rotating machinery.

WEIPING ZHAO received the B.S. degree from the Zhongyuan University of Technology, in 2015. She is currently pursuing the Ph.D. degree with the School of Energy, Power, and Mechanical Engineering, North China Electric Power University. Her research interests include contamination deposition characteristics of insulators and monitor of dust deposition on solar photovoltaic panels.

QINGZHUANG SONG was born in Xuzhou, China, in 1994. He is currently pursuing the M.S. degree with the Department of Power Engineering, North China Electric Power University, China. His research interest includes the contamination deposition characteristics of insulator.